

Photon emission from collisional excitation of N_2O by 100–325-keV H^+

Michael N. Monce

Department of Physics and Astronomy, Connecticut College, New London, Connecticut 06320

(Received 12 May 1986)

Nitrous oxide was bombarded with protons with an energy range of 100–325 keV. The photon emission from collisional excitation of the N_2O in the wavelength range of 2000–7000 Å was examined. The only spectral features found were from transitions from the $A^2\Sigma^+$ state to the $X^2\Pi$ state of N_2O^+ . The emission cross sections for the four most prominent bands were measured. The resulting cross-section data do not make a distinction between the Bethe-Born theory and the impact-parameter model.

I. INTRODUCTION

The subject of photon emission resulting from collisions between ions and diatomic molecules has been studied thoroughly.^{1,2} However, there appears to be very little data regarding these processes in connection with polyatomic molecules, especially in the intermediate bombarding energy range of 100–500 keV. Also, as noted by several researchers,^{3,4} no detailed theoretical calculations exist concerning these collisions. Thus, experimental data is needed, especially with regard to photon-emission cross sections. Besides the interest in the physics of ion-molecule collisions, the data on photon emission from such collisions could be useful in other areas such as the study of the upper atmosphere of planets where there is bombardment by high-energy ions from the solar wind.

The photon emission from collisions of ions with nitrous oxide has been studied up to the collisional energy of 25 keV.^{5–8} This paper reports data on photon emission resulting from collisions between protons with energies between 100 and 325 keV, and N_2O . Nitrous oxide is isoelectronic with CO_2 . Thus, comparison can also be made to studies where CO_2 was the target molecule.^{9,10}

II. EXPERIMENTAL PROCEDURE

As this is the first paper from this laboratory the experimental apparatus and procedure will be described in detail.

A. Apparatus

The beam of protons for this work was obtained from the Connecticut College Van de Graaff accelerator. The accelerator has a maximum terminal voltage of 400 kV and a practical working range of 100–325 keV. The beam is mass and energy analyzed by a 90° magnet. The uncertainty in beam energy is less than 1%.

As shown in Fig. 1, the beam enters a differentially pumped collision chamber where it is collimated to a diameter of approximately 3 mm. After passing through a target gas cell the beam is collected by a Faraday cup. A guard ring in front of the Faraday cup is kept at a potential of –100 V to suppress secondary electron emission.

The target gas cell is shown in Fig. 2. The target gas enters the cell through the tube at the top. The tube at the bottom is connected to an MKS Instruments capacitance manometer. The gas pressure is controlled through the use of a precision needle valve. Also placed inside the cell is a thermistor for temperature measurement. The thermistor was calibrated using a 0.1°C mercury thermometer. The beam path length through the cell is 3 cm. The viewing slit along the beam path is 0.5 cm wide.

Photons that are emitted at 90° to the beam direction are collected and collimated by a cylindrical lens placed a focal length away from the beam path. After passing through a uv grade polarizer the photons are focused onto the 150- μm entrance slit of a 0.25-m Jarrell-Ash monochromator. The photons are detected by a Hamamatsu

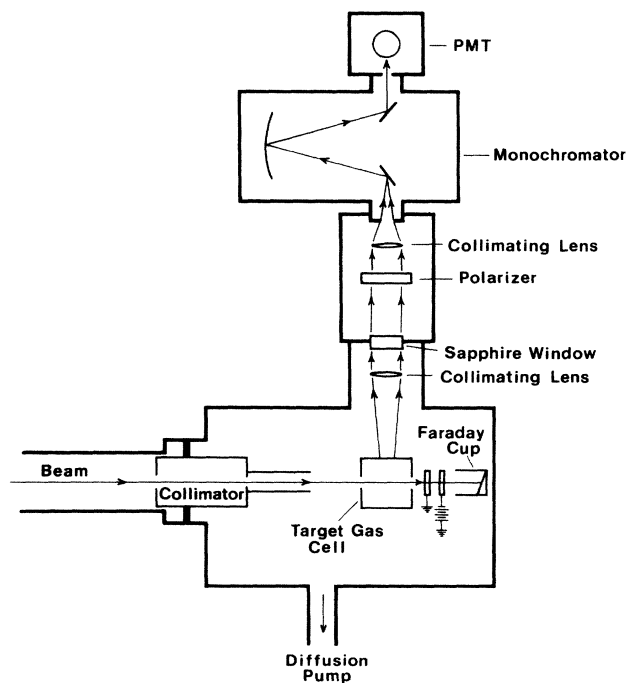


FIG. 1. Schematic drawing of the collision chamber and the photon detection system.

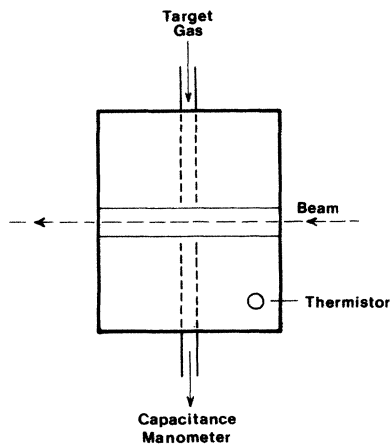


FIG. 2. Schematic drawing of the target gas cell.

R955 photomultiplier tube (PMT) cooled to a temperature of approximately -25°C and placed at the exit slit of the monochromator.

A block diagram of the electronics used is shown in Fig. 3. The scan drive on the monochromator has a 0–4 V dc output which is proportional to wavelength. By gating this signal with the PMT output it is possible to generate a spectrum in the multichannel analyzer memory. The data is transferred from the multichannel analyzer (MCA) to a microcomputer for analysis.

B. Sensitivity and wavelength calibration

The optical system was calibrated in terms of wavelength by inserting a mercury discharge lamp in the target gas cell. A spectrum was then generated and a correlation made between channel number and wavelength. The monochromator contains two gratings; one for the wavelength region of 2000–4000 Å, and one for 4000–7000 Å. Wavelength calibration was carried out for both gratings and for a number of analog-to-digital converter (ADC) settings on the multichannel analyzer.

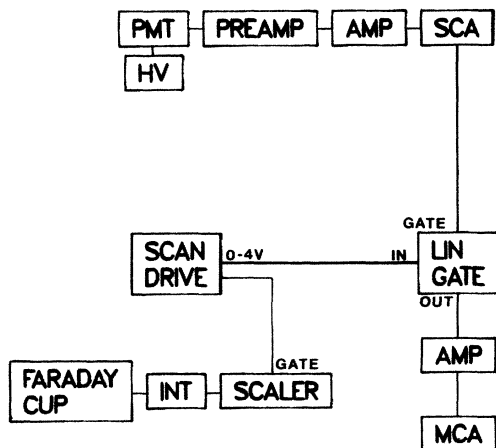


FIG. 3. Block diagram of the electronics used in this experiment.

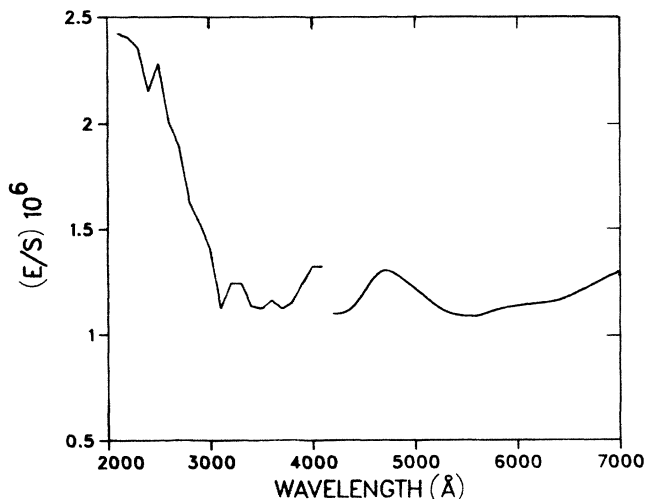


FIG. 4. Correction function for the optical sensitivity of the system for photons polarized parallel to the beam direction. E/S is the ratio of the spectral radiance of the standard lamp to the measured lamp emission. The uncertainty in the measurement is 14%. The discontinuity at 4000 Å is due to a change of monochromator gratings.

Following the procedure outlined by Thomas,² the variation of the sensitivity of the optical system with wavelength was measured.

For the visible region (4000–7000 Å), a tungsten-halogen lamp was placed in the target cell with its filament aligned along the beam path. The intensity of the lamp as a function of wavelength was measured using a National Bureau of Standards (NBS) calibrated spectrophotometer.

For the ultraviolet region (2000–4000 Å) a deuterium lamp was placed in the target cell. The deuterium lamp

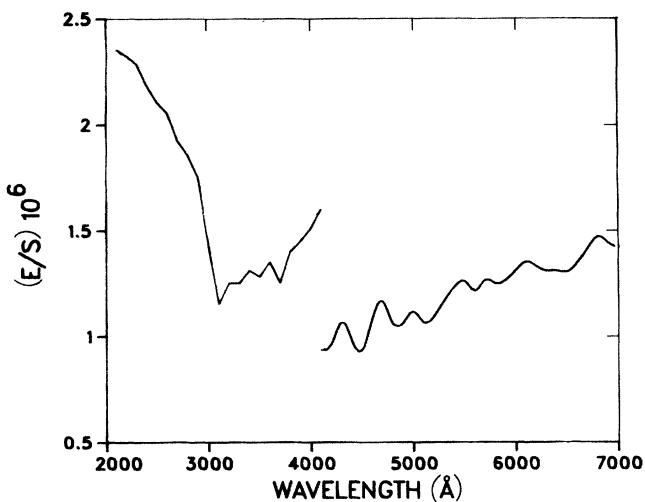


FIG. 5. Correction function for the optical sensitivity of the system for photons polarized perpendicular to the beam direction. E/S is the ratio of the spectral radiance of the standard lamp to the measured lamp emission. The uncertainty in the measurement is 14%. The discontinuity at 4000 Å is due to a change of monochromator gratings.

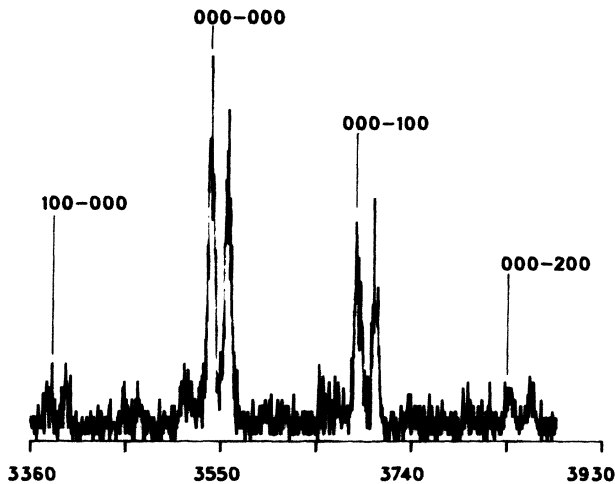


FIG. 6. Typical spectrum of photon emission arising from collisions of H^+ on N_2O . Wavelength units are in angstroms. The four major transitions from the $A^2\Sigma^+ - X^2\Pi$ system are identified.

has a continuous spectrum in the uv region. Its intensity was measured using a NBS traceable standard by a commercial laboratory.

In each case (uv and visible) a spectrum for the lamp was generated. A neutral density filter was inserted in front of the photomultiplier tube cathode to decrease the intensity of the light. The variation of the optical density of the filter with wavelength was known and corrected for in generating the observed spectrum for each lamp. The known spectral radiance for the lamp was divided by the observed intensity per angstrom bandwidth to yield a correction function for the optical system. This is displayed in Figs. 4 and 5. A correction function was generated for both photons polarized parallel and perpendicular to the beam direction. It will be noted that below

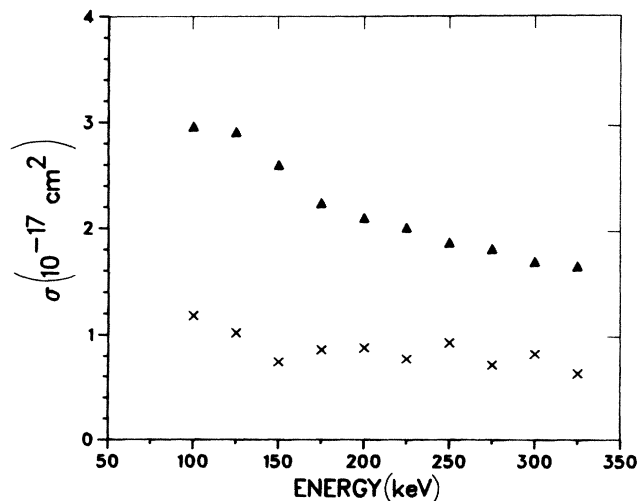


FIG. 7. Photon-emission cross sections as a function of proton energy. Δ , (000-000) transition; \times , (000-200) transition. Uncertainty in the data is 20%.

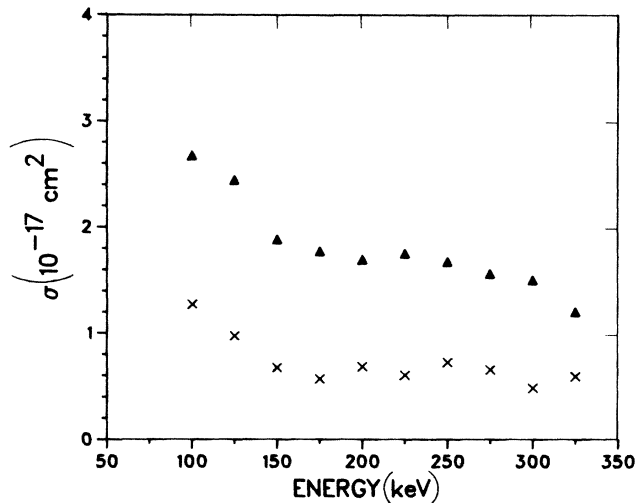


FIG. 8. Proton-emission cross sections as a function of proton energy. Δ , (000-100) transition; \times , (100-000) transition. Uncertainty in the data is 20%.

3000 Å the correction function increases rapidly. This can be totally accounted for by a decrease in transmission of both the monochromator grating and the polarization filter.

The small variations seen in the correction curves, especially those in the visible region in Fig. 5, are probably due to spurious secondary reflections within the monochromator. When such variations are taken into account, the uncertainty in the correction functions is estimated to be 14%.

In order to make the sensitivity corrections, and hence the measured emission cross sections, absolute, cross-section data were taken for the 3914 Å band of N_2^+ ($0-0, B^2\Sigma_u^+ - X^2\Sigma_g^+$) produced in collisions of 100-keV protons with N_2 . Hoffman *et al.* have made a very precise determination of this cross section for use as a standard.¹¹ The correction function was adjusted by 0.62 to normalize to

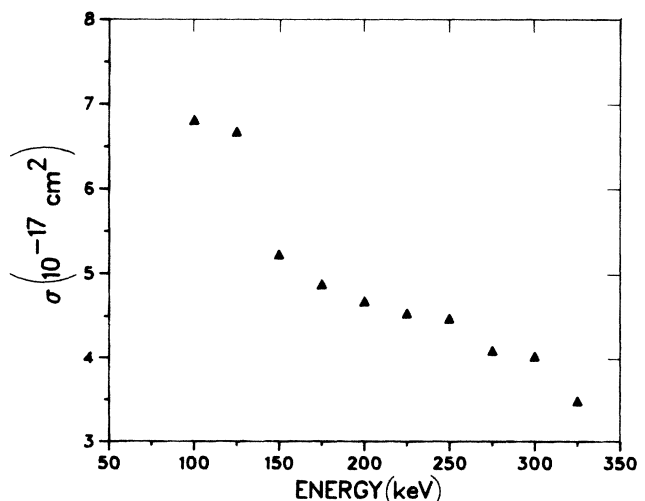


FIG. 9. Photon-emission cross sections as a function of proton energy for the total of the 000- n 00 transitions, $n=0,1,2$. Uncertainty in the data is 20%.

TABLE I. Photon-emission cross sections. Units are 10^{-17} cm², uncertainty 20%.

H ⁺ energy (keV)	Cross sections (10^{-17} cm ²)				total 000- <i>n</i> 00	100-000
	000-000	Transition		000-200		
100	2.96	000-100	2.67	1.18	6.81	1.27
125	2.91		2.44	1.02	6.67	0.97
150	2.60		1.88	0.74	5.22	0.67
175	2.24		1.77	0.86	4.87	0.56
200	2.10		1.69	0.88	4.67	0.68
225	2.01		1.75	0.77	4.53	0.60
250	1.87		1.67	0.93	4.47	0.72
275	1.81		1.56	0.71	4.08	0.65
300	1.69		1.50	0.82	4.01	0.48
325	1.65		1.20	0.63	3.48	0.6

the value given by Hoffman *et al.* Following this measurement, the cross section of the 4278-Å band of N₂⁺ (0-1, B²Σ_u⁺ - X²Σ_g⁺) was measured. This band has been shown to be 0.35 times the intensity of the 3914-Å band both theoretically and experimentally.¹² The correction function for the visible region was then adjusted by 0.33 to yield the correct ratio for the intensity of the 4278-Å band to the 3914-Å band.

C. Procedure

In measuring an emission cross section for a particular band several scans were made for both photons polarized perpendicular and parallel to the beam direction. This allowed correction for any anisotropy of the radiation due to polarization and also corrected for error in instrument sensitivity due to polarization.²

High- and low-wavelength limit controls on the monochromator were used to bracket a wavelength region of interest. When the monochromator scanned between these limits a gating signal was sent to the current integrator. Thus, the beam current was measured simultaneously as the monochromator scanned through the spectral band that was being investigated. Pressure and temperature were also recorded at this time.

For each scan the peak due to photon emission was integrated and background subtracted. A computer program calculated the resulting emission cross section from the raw data after applying the correction factors for sensitivity. The target gas density was calculated via the ideal gas law.

To establish the range of single-collision conditions a measurement of the photon-emission intensity versus the target gas pressure was made. For the N₂O target it was found that this function was linear up to a pressure of 5 m Torr. All subsequent measurements were done at a pressure of 3 m Torr. Typical beam currents were on the order of 0.4 μA. Background pressure was generally less than 8×10^{-6} Torr.

III. RESULTS

A typical photon-emission spectrum arising from collisions of protons with N₂O is shown in Fig. 6. The

features shown are identified as arising exclusively from the A²Σ⁺ - X²Π system of N₂O⁺.¹³ There was no evidence of any other emissions in the wavelength region of 2000-7000 Å. This is consistent with the findings of other workers at different energies.⁵⁻⁸

The spectrum is dominated by four double-headed bands arising from 100-000 and 000-*n*00 transitions, *n*=0,1,2.

Emission cross sections for these four bands were measured as a function of proton energy. The results are shown in Figs. 7-9 and are listed in Table I. The estimated uncertainty of the cross-section measurements is 20%.

IV. DISCUSSION

The lack of other emission features in the spectrum does not preclude the existence of other excitation processes, especially that of dissociation. For collisions of 1-MeV H⁺ with N₂O, Shah *et al.*¹⁴ have shown the existence of singly ionized dissociative fragments. Also, through coincidence measurements, it was argued that these fragments were emerging in the ground state.¹⁵ At the lower energy of 25-keV H⁺, Birely and Johnson reported several atomic nitrogen and oxygen lines in the infrared.⁷

However, this study and others⁵⁻⁸ show that the dominant process involving photon emission appears to be excitation to the A²Σ⁺ state of N₂O⁺. This perhaps can be understood by examining the electronic structure of the molecule. The three outer valence orbitals of N₂O are¹³

$$K 1\pi^4 7\sigma^2 2\pi^4 .$$

Whereas, the A²Σ⁺ state of the N₂O⁺ involves the removal of a single 7σ electron:

$$K 1\pi^4 7\sigma 2\pi^4 .$$

Callomon and Creutzberg¹³ argue that the 2π electrons are highly localized on the oxygen atom, while the 1π electrons are bonding and the 7σ electrons are a lone pair. Removal of a 2π electron is less probable due to localization, while removal of a 1π electron involves excitation to the B²Π state of N₂O⁺ which is strongly predissociative.

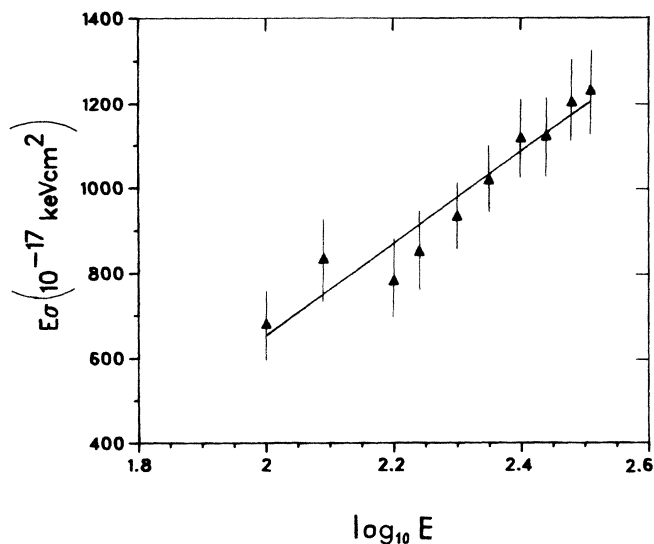


FIG. 10. Fano plot of the total photon-emission cross section for the 000- $n00$, $n=0,1,2$ transitions. Best fit line was determined by the linear least-squares method.

Thus, removal of a single 7σ electron may be the most probable nondissociative channel.

If the above analysis is correct, then the emission cross sections measured for the $A^2\Sigma^+ - X^2\Pi$ transitions may also represent excitation cross sections. Thus, it should be possible to fit the cross-section data to a theoretical model. Both Moore⁶ and Birely and Johnson,⁵ show through energy-defect arguments, that in the H^+ energy range of 0.7–25 keV the adiabatic approximation does not adequately describe the observed emissions. Thus, it could be expected that a high-energy-limit approach such as the impact-parameter method or the Bethe-Born approximation would be applicable especially in the range of 100–325 keV.

The data of Rudd *et al.*,⁹ for a CO_2 target, shows that for the total ionization cross section, σ_+ , the Bethe-Born theory gives good agreement with the data down to a proton energy of 10 keV. This suggests that a similar approach could be taken with N_2O . A Fano plot of the total emission cross section for the 000- $n00$ transitions, $n=0,1,2$, from the present study is shown in Fig. 10. In the Bethe-Born model this should approach a straight line.¹⁶ The average deviation of the data from the best fit line shown is 7%.

In the limit of large projectile velocities (compared to the electron orbital velocity) the cross section in the impact parameter method is given by¹⁷

$$\sigma \sim \frac{1}{v^2}. \quad (1)$$

Shown in Fig. 11 is the total emission cross section for

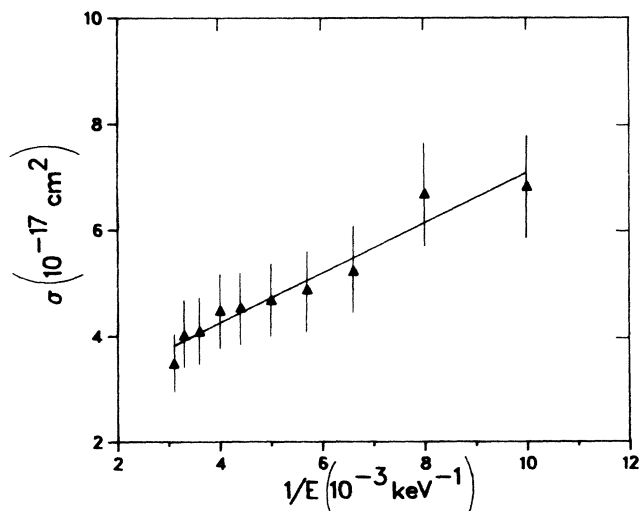


FIG. 11. Plot of the total photon-emission cross section for the 000- $n00$ transitions, $n=0,1,2$, as a function of $1/E$. Best fit line was determined by the linear least-squares method.

the 000- $n00$ transitions now plotted as a function of $1/E$. This also shows a linear relation, as predicted by Eq. (1), with an average deviation from the best fit of 5%. Thus, over the relatively narrow energy range of the data presented here it is impossible to make a distinction between the impact parameter theory and the Bethe-Born theory at least for excitation to the 000, $A^2\Sigma^+$ level of N_2O^+ . Analysis for the 100- $n00$ transitions was not carried out because of the difficulty of measuring the cross sections for the 100-100, 100-200, etc. transitions.

Obviously much more data are needed with regard to these collisions especially in the energy ranges of 25–100 keV and from 300 keV up. Nitrous oxide may be a particularly useful target for investigating these collision processes due to its relatively simple emission spectrum. This can be contrasted to CO_2 which shows numerous emissions from the excited parent molecule in both neutral and singly ionized forms, as well as emissions from various dissociative fragments.¹⁰ Work is continuing at this laboratory on N_2O using He^+ projectiles, and with other polyatomic targets.

ACKNOWLEDGMENT

The author would like to thank Brad Dinerman for his assistance in the data collection. Also a debt is owed to the U.S. Coast Guard Research and Development Center, Groton, CT, for their assistance in calibrating the tungsten lamp. This work is supported by a Cottrell College grant from the Research Corporation.

¹J. T. Park, *Collisional Spectroscopy*, edited by R. G. Cooks (Plenum, New York, 1978), Chap. 1.

²E. W. Thomas, *Excitation in Heavy Particle Collisions* (Wiley-Interscience, New York, 1972).

³M. E. Rudd, T. V. Goffe, and A. Itoh, *Phys. Rev. A* **32**, 2128 (1985).

⁴M. Kimura, *Phys. Rev. A* **32**, 802 (1985).

⁵J. H. Birely and P. A. Johnson, *J. Chem. Phys.* **62**, 4854 (1975).

- ⁶J. H. Moore, *J. Geophys. Res.* **80**, 3727 (1975).
- ⁷D. H. Loyd and H. R. Dawson, *Phys. Rev. A* **19**, 948 (1979).
- ⁸M. Haugh, T. G. Slanger, and K. D. Bayes, *J. Chem. Phys.* **44**, 837 (1966).
- ⁹M. E. Rudd, R. D. Dubois, L. H. Toburen, C. A. Ratcliffe, and T. V. Goffe, *Phys. Rev. A* **28**, 3244 (1983).
- ¹⁰M. C. Poulizac and M. Dufay, *Astrophys. Lett.* **1**, 17 (1967).
- ¹¹J. M. Hoffman, G. J. Lockwood, and G. H. Miller, *Phys. Rev. A* **11**, 841 (1975).
- ¹²E. W. Thomas, G. D. Bent, and J. L. Edwards, *Phys. Rev.* **165**, 32 (1968).
- ¹³J. H. Callomon and F. Creutzberg, *Philos. Trans. R. Soc. (London)* **277**, 157 (1974).
- ¹⁴A. V. Shah, M. N. Monce, A. K. Edwards, M. F. Steuer, and R. M. Wood, *J. Chem. Phys.* **73**, 6174 (1980).
- ¹⁵A. V. Shah, doctoral dissertation, University of Georgia, 1981 (unpublished).
- ¹⁶M. Inokuti, *Rev. Mod. Phys.* **43**, 297 (1971).
- ¹⁷R. E. Johnson, *Introduction to Atomic and Molecular Collisions* (Plenum, New York, 1982), Chap. 4.